BJP British Journal of Pharmacology

DOI:10.1111/bph.13127
www.brjpharmacol.org

RESEARCH PAPER

Effect of tyrphostin AG879 on $K_v4.2$ and $K_v4.3$ potassium channels

Haibo Yu[1,2], Beiyan Zou[2]*, Xiaoliang Wang[1] and Min Li[2†]

[1]*State Key Laboratory of Bioactive Substances and Functions of Natural Medicines, Institute of Materia Medica, Chinese Academy of Medical Sciences and Peking Union Medical College, Beijing, China, and* [2]*The Solomon H. Snyder Department of Neuroscience, High Throughput Biology Center and Johns Hopkins Ion Channel Center, Johns Hopkins University, Baltimore, MD, USA*

Correspondence
Haibo Yu, State Key Laboratory of Bioactive Substances and Functions of Natural Medicines, Institute of Materia Medica, Chinese Academy of Medical Sciences and Peking Union Medical College, Beijing, China.
E-mail: haiboyu@imm.ac.cn

*Present address: Molecular Devices LLC, Sunnyvale, CA 94089, USA.

†Present address: GlaxoSmithKline, 709 Swedeland Road, King of Prussia, PA 19406, USA.

Received
18 September 2014
Revised
25 February 2015
Accepted
2 March 2015

BACKGROUND AND PURPOSE

A-type potassium channels (I_A) are important proteins for modulating neuronal membrane excitability. The expression and activity of $K_v4.2$ channels are critical for neurological functions and pharmacological inhibitors of $K_v4.2$ channels may have therapeutic potential for Fragile X syndrome. While screening various compounds, we identified tyrphostin AG879, a tyrosine kinase inhibitor, as a $K_v4.2$ inhibitor from. In the present study we characterized the effect of AG879 on cloned $K_v4.2$/K_v channel-interacting protein 2 (KChIP2) channels.

EXPERIMENTAL APPROACH

To screen the library of pharmacologically active compounds, the thallium flux assay was performed on HEK-293 cells transiently-transfected with $K_v4.2$ cDNA using the Maxcyte transfection system. The effects of AG879 were further examined on CHO-K1 cells expressing $K_v4.2$/KChIP2 channels using a whole-cell patch-clamp technique.

KEY RESULTS

Tyrphostin AG879 selectively and dose-dependently inhibited $K_v4.2$ and $K_v4.3$ channels. In $K_v4.2$/KChIP2 channels, AG879 induced prominent acceleration of the inactivation rate, use-dependent block and slowed the recovery from inactivation. AG879 induced a hyperpolarizing shift in the voltage-dependence of the steady-state inactivation of $K_v4.2$ channels without apparent effect on the $V_{1/2}$ of the voltage-dependent activation. The blocking effect of AG879 was enhanced as channel inactivation increased. Furthermore, AG879 significantly inhibited the A-type potassium currents in the cultured hippocampus neurons.

CONCLUSION AND IMPLICATIONS

AG879 was identified as a selective and potent inhibitor the $K_v4.2$ channel. AG879 inhibited $K_v4.2$ channels by preferentially interacting with the open state and further accelerating their inactivation.

Abbreviations

KChIP2, K_v channel-interacting protein 2; KO, knock-out; PTK, protein tyrosine kinase

Tables of Links

TARGETS		
Ion channels[a]		**Catalytic receptors**[b]
$K_v1.1$	$K_v2.1$	ErbB2 receptor (HER2)
$K_v1.3$	$K_v4.2$	TrkA
$K_v1.4$	$K_v4.3$	VEGFR-2 (FLK-1)
$K_v1.5$		

LIGANDS
Genistein
Tyrphostin AG879

These Tables list key protein targets and ligands in this article which are hyperlinked to corresponding entries in http://www.guidetopharmacology.org, the common portal for data from the IUPHAR/BPS Guide to PHARMACOLOGY (Pawson *et al.*, 2014) and are permanently archived in the Concise Guide to PHARMACOLOGY 2013/14 ([a,b]Alexander *et al.*, 2013a,b).

Introduction

A-type potassium channels (I_A) are important proteins with a variety of functional roles in modulating neuronal membrane excitability (Hoffman *et al.*, 1997; Birnbaum *et al.*, 2004; Kim *et al.*, 2005; Yuan *et al.*, 2005). Several cloned K_v channels, including $K_v4.2$, $K_v4.3$ and $K_v1.4$, exhibit transient, rapidly activating A-type currents when expressed in heterologous systems. Recent experiments using knock-out (KO) mice with a targeted disruption of the $K_v4.2$ gene ($K_v4.2^{-/-}$) have revealed that $K_v4.2$ is the major subunit contributing to I_A in hippocampal and cortical pyramidal neurons, as well as in dorsal horn neurons of the spinal cord (Chen *et al.*, 2006; Hu *et al.*, 2006; Norris and Nerbonne, 2010). *$K_v4.2$* KO mice exhibit pronounced defects in performing hippocampus-dependent learning and memory tasks (Lugo *et al.*, 2012; Truchet *et al.*, 2012). The localization of $K_v4.2$ channels at synapses and their ability to regulate neuron firing support a role for these channels in modulating synaptic activity in the hippocampus and influencing hippocampus-dependent tasks (Chen *et al.*, 2006). These studies have provided compelling evidence that the expression and activity of $K_v4.2$ channels are critical for neurological functions.

Recent studies have shown that the expression of $K_v4.2$ channels is markedly increased in FMR1 (coding for fragile X mental retardation protein) KO mice that lack fragile X mental retardation protein, a Fragile X syndrome (FXS) model (Lee *et al.*, 2011). Furthermore, the defective long-term potentiation (LTP) induced in hippocampus slices from FMR1 KO mice can be restored by reducing K_v4 channel activity. Therefore, pharmacological inhibitors of $K_v4.2$ may be considered for potential therapeutic applications. However, only a few pharmacological gating modifiers of $K_v4.2$ have been reported (Tseng *et al.*, 1996; Sanguinetti *et al.*, 1997; Diochot *et al.*, 1999; Ebbinghaus *et al.*, 2004). There is still a need to identify more $K_v4.2$ inhibitors, which may be used to analyse mental retardation in which $K_v4.2$ channels are involved and could potentially serve as lead compounds for the development of new treatments. We screened a 1280 compound library on $K_v4.2$ potassium channels. Tyrphostin AG879, a protein tyrosine kinase (PTK) inhibitor, appeared to be the most potent compound. Here we mainly studied the effects of AG879 on $K_v4.2$ channels co-expressed with Kv channel-interacting protein 2 (KChIP2), an accessory subunit. The possible mechanism of the inhibitory effect of AG879 is also discussed.

Methods

Cell culture and transient transfection

HEK-293 and CHO-K1 cells were routinely cultured in either DMEM or 50/50 DMEM/F-12 (Mediatech, Manassas, VA, USA), supplemented with 10% FBS (Gemini Bio-products, West Sacramento, CA, USA) and 2 mM L-glutamine (Invitrogen, Carlsbad, CA, USA). Cells were maintained and passaged when reaching 80% confluence.

For the thallium-based assay, HEK-293 cells were transfected with the $K_v4.2$-pcDNA3.1 plasmid with MaxCyte STX® Scalable Transfection System (MaxCyte, Gaithersburg, MD, USA) to achieve a consistent expression level. For the patch-clamp recording, CHO-K1 cells were transfected with $K_v4.2$ or $K_v4.2$/KChIP2 plasmids using Lipofectamine™ LTX with Plus™ Reagent according to the manufacture's instruction (Invitrogen). Plasmid containing EGFP was co-transfected to identify transfection-positive cells as a marker. After transfection for 24 h, the cells were split and replated onto coverslips coated with poly-L-lysine (Sigma, St. Louis, MO, USA) for electrophysiological recording.

Hippocampus neuron culture

The neuronal culture method was adopted and modified from a protocol described previously (Ahlemeyer and Baumgart-Vogt, 2005). The study was approved by the Institutional Animal Care and Use Committee at the Chinese Academy of Medical Sciences (CAMS) and was performed in accordance with the National Institute of Health Guide for the care and use of laboratory animals. All studies involving animals are reported in accordance with the ARRIVE guidelines for reporting experiments involving animals (Kilkenny *et al.*, 2010; McGrath *et al.*, 2010). Pregnant Sprague-Dawley rats were killed by an overdose of isoflurane at embryonic day 18. For the experiment, a total of 10 fetal rats were used for hippocampus neuron dissection. The uterus was dissected out and placed in a sterile Petri dish. The fetuses were removed from the uterus and hippocampus tissues were dissected out from their brains. The tissue was digested with 0.25% Trypsin and resuspended into single cells. The single-cell suspension was plated on poly-D-lysine–coated coverslips. The neurons were maintained in culture medium consisting of neurobasal medium with B-27 supplement (Invitrogen), penicillin, streptomycin and 2 mM L-glutamine. Cultured neurons on day 10–14 were used for electrophysiological recording.

Thallium-based fluorescence assay

The library of pharmacologically active compounds (LOPAC) (Sigma-Aldrich) was chosen to screen for $K_v4.2$ inhibitors. HEK-293 cells expressing $K_v4.2$ were used. The activity of $K_v4.2$ potassium channels was monitored by the influx of a surrogate ion for potassium, thallium (Tl^+). Thallium influx was detected through the use of a thallium-sensitive fluorescent dye, FluxOR™ (Invitrogen). Cells were seeded at 6500 cells per well into BD Biocoat 384-well-plates (poly-D-Lysine coated) and incubated overnight at 37°C and 5% CO_2. On the day of assay, medium was removed; cells were incubated with 1× FluxOR solution for 90 min at room temperature (RT) in the dark; the 1× FluxOR solution was replaced by assay buffer (HBSS containing 5.8 mM potassium; Catalogue # 14065, Invitrogen); test compounds 10 μM were then added to cells and incubated for 20 min; cell plates were loaded onto a Hamamatsu FDSS 6000 kinetic imaging plate reader (Hamamatsu Photonics, Hamamatsu City, Japan); after the establishment of a fluorescence baseline by 1 Hz scanning for 10 s, the $K_v4.2$ channels were activated with a stimulus buffer containing 2.5 mM K_2SO_4 and 12 mM Tl_2SO_4 giving a final potassium concentration of 10.8 mM and final Tl^+ concentration of 24 mM; fluorescence measurement was continued at 1 Hz for another 110 s. The fluorescence ratio, F(max–min)/F0 (F/F0), was calculated for each well using the entire 120 s detection window and then normalized to the positive and negative control wells. Compared with negative controls, if a compound caused the signal to decrease by more than three times the standard deviation (SD) of the fluorescence ratio, it was classified as an inhibitor.

Electrophysiological recordings

Traditional whole-cell voltage-clamp recordings were performed at RT to record the $K_v4.2$ and $K_v4.2$/KChIP2 currents of the transiently transfected CHO-K1 cells. Transfected cells were dissociated and seeded onto glass coverslips at a low density on the day of recording. Recording pipettes were pulled with borosilicate glass (World Precision Instruments, Inc., Sarasota, FL, USA) to 2–5 MΩ when filled with a pipette solution containing 145 mM KCl, 1 mM $MgCl_2$, 5 mM EGTA, 10 mM HEPES and 5 mM MgATP at pH 7.2 and placed in a bath solution containing 140 mM NaCl, 5 mM KCl, 2 mM $CaCl_2$, 1.5 mM $MgCl_2$, 10 mM glucose and 10 mM HEPES at pH 7.4 adjusted with NaOH. Isolated cells were voltage-clamped in whole-cell mode with an AxoPatch 200B amplifier (Molecular Devices Corporation, Sunnyvale, CA, USA), and currents were recorded at 10 kHz. Cells were continuously perfused with bath solution through a gravity-driven perfusion system (ALA Scientific, Farmingdale, NY, USA). Stock solutions of test drugs were made with DMSO. Immediately before each experiment, drugs were diluted in appropriate external solutions to the desired concentrations and applied by perfusion. Recordings were performed at RT (22–25°C).

Chemicals

The library of pharmacologically active compounds (LOPAC), genistein and sodium orthovanadate were obtained from Sigma-Aldrich (St. Louis, MO, USA). Tyrphostin AG879 was from Selleck (Chemicals (Houston, TX, USA); the compound stock was prepared in DMSO at 30 mM.

Data analysis

The data from the thallium-based flux assay were analysed by the manufacturer's software package (Hamamatsu Photonics). Patch-clamp data were processed in Clampfit 9.2 (Molecular Devices,Sunnyvale, CA, USA) and then analysed in Excel and Origin 6.0 (OriginLab Corporation, Northampton, MA, USA). Dose–response curves were fitted by the Hill equation in Origin software: $Y = 1/[1 + (IC_{50}/C)^P]$, where Y is the fractional block at drug concentration C; IC_{50} the drug concentration producing half of the maximum block; and P the Hill coefficient. The steady-state activation and inactivation curves were fitted with the Boltzmann equation $G = 1/[1 + \exp(V - V_{1/2})/S]$. $V_{1/2}$ is the voltage needed to open half of the total number of channels and S is the slope factor. The voltage-dependence of the fractional block was fitted to the Woodhull equation (Woodhull, 1973): $f = [D]/[[D] \mid K_d(0)e^{-z\delta FV/RT}]$, where K_d represents the binding affinity at the reference voltage (0 mV); δ is the fractional electrical distance (the fraction of the transmembrane electrical field sensed by a single charge at the receptor site); z is the charge valence of the compound; F is the Faraday constant; V is the test potential; R is the universal gas constant; T is absolute temperature.

Statistics

Data were summarized as the mean ± SEM. Student's t-test was used for statistical analysis. $P < 0.05$ was considered statistically significant.

Results

Identification of tyrphostin AG879 as a selective $K_v4.2$ inhibitor

A High throughput screen was done using HEK-293 cells that were transiently transfected with rat $K_v4.2$ plasmid using the Maxcyte transfection system. Here HEK-293 cells were well-optimized for the transfection system. LOPAC was screened at 10 μM in duplicate using the optimized conditions (see Methods). Among the screened plates in duplicate, the Z′ factor was 0.52 ± 0.05 (n = 8), a robust range for a cell-based high-throughput screen campaign. Supporting Information Figure S1 shows the comparison of two repeats with $R^2 = 0.95$, indicative of an excellent correlation between the different experiments when the same compounds were tested. A screening of 1280 known bioactive compounds yielded 11 compounds that inhibited $K_v4.2$-mediated Tl^+ influx when a criterion of five times the SD value or more decrease in activity in comparison with the mean of buffer controls was used, with a cut-off at 10 μM, and six of these compounds were confirmed in the Tl^+ assay. Then we examined their effects on $K_v4.2$ channels using electrophysiological recordings.

Among all of the compounds tested, tyrphostin AG879, a tyrosine kinase inhibitor of the nerve growth factor receptor, ErbB2 (Snyders *et al.*, 1992; He *et al.*, 2004; Zhou and Brattain, 2005), was confirmed and appeared to be the most potent $K_v4.2$ inhibitor. Its chemical structure and inhibitory effect are shown in Figure 1A and B. For the whole-cell patch-clamp experiments, CHO-K1 cells were used for transient transfection. As shown in Supporting Information Figure S2, the $K_v4.2$ channel alone expressed in CHO-K1 cells displayed a

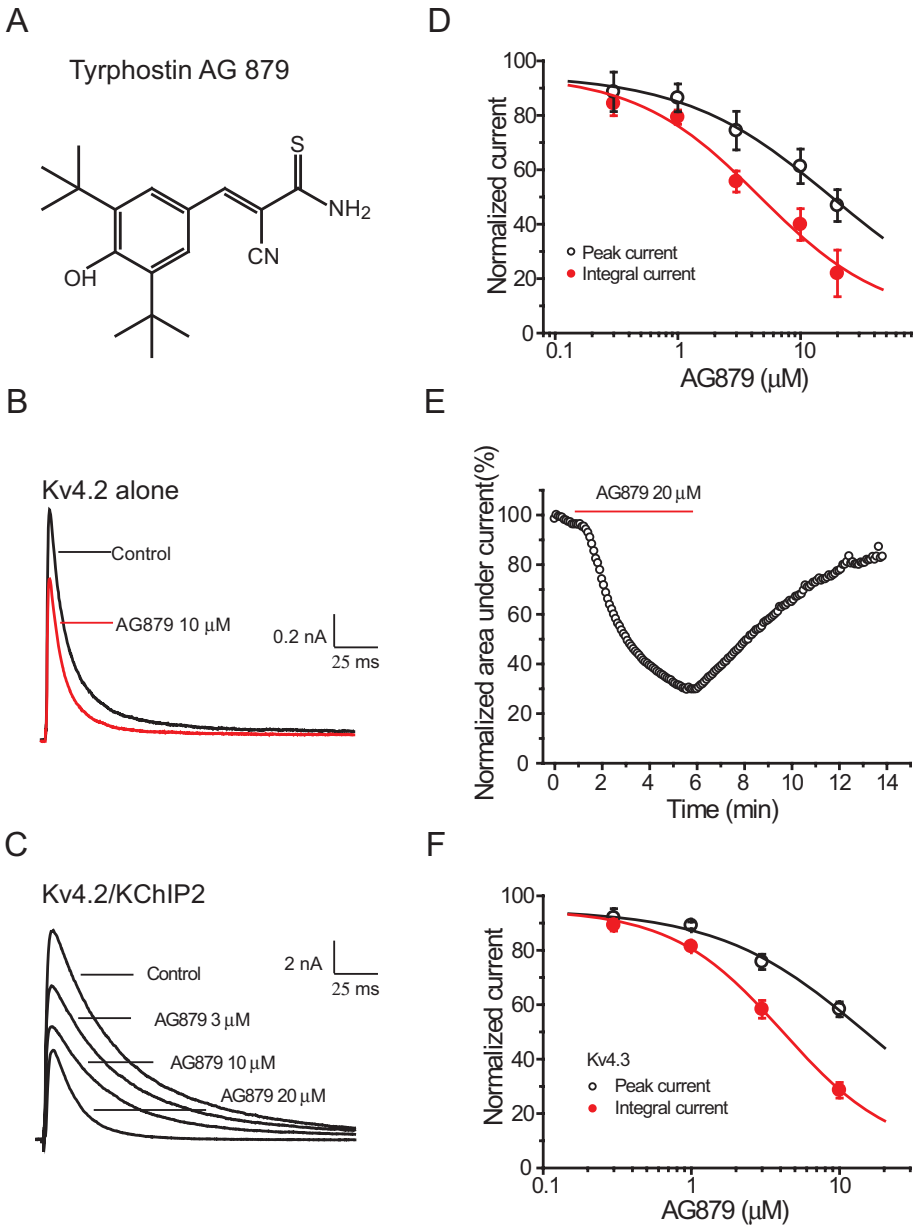

Figure 1

Identification of tyrphostin AG879 as a $K_v4.2$ channel inhibitor. (A) Chemical structure of AG879. (B) Effect of AG879 on $K_v4.2$ channels in CHO-K1 cells. AG879 10 μM reduced the $K_v4.2$-mediated peak current by 31.27 ± 2.4%. The $K_v4.2$ channel currents were recorded by a depolarization to +40 mV for 300 ms from a holding potential −80 mV. (C) Inhibition by AG879 3, 10 and 20 μM of $K_v4.2$/KChIP2 co-expressed channels. (D) Concentration-dependent inhibition by AG879 of $K_v4.2$/KChIP2 channel shown by measuring peak and integral currents. Concentration–response curves for AG879 were fitted to the Hill equation. (E) Reversible inhibition of $K_v4.2$ by AG879. Maximal inhibition occurred ~5 min after drug application. (F) Concentration-dependent inhibition by AG879 of $K_v4.3$ channels.

medium expression level and fast inactivation kinetics. As reported previously (An *et al.*, 2000), K_v channel-interacting protein 2 (KChIP2), one of the KChIPs, is associated and co-localized with $K_v4.2$ in the CNS resulting in increased surface expression, slower inactivation and accelerated recovery from inactivation. To mimic the native channel complex and improve the expression level of $K_v4.2$ channels, we co-trasfected cDNAs of $K_v4.2$ and KChIP2 to study the effect of $K_v4.2$ inhibitors. Consistent with earlier reports, co-expression of $K_v4.2$ with KChIP2 increased the amplitude of the $K_v4.2$-mediated current by more than 15-fold when peak currents were measured. And the inactivation phase was also slowed (Supporting Information Figure S2C).

As shown in Figure 1B and C, AG879 10 μM induced similar levels of inhibition when the peak currents for both $K_v4.2$ alone and $K_v4.2$/KChIP2-coexpressed channels were measured. Thus, the $K_v4.2$/KChIP2 channel complex was used to explore the effect of AG879. When cells were depo-

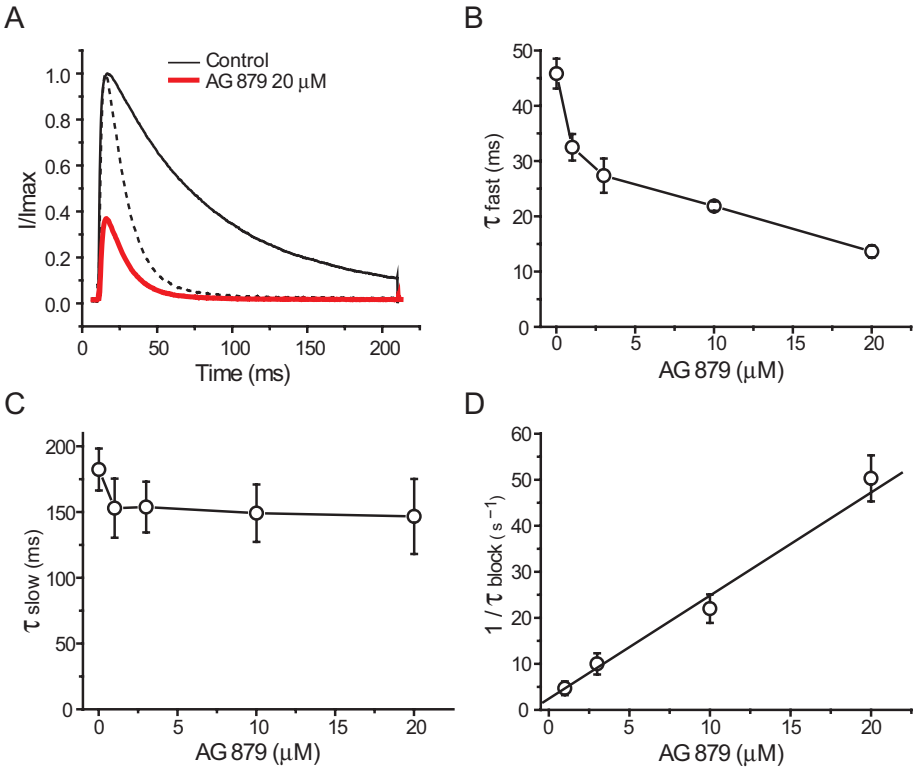

Figure 2

Effect of AG879 on the inactivation time course. (A) $K_v4.2$ currents were activated by depolarization pulses from –80 to +40 mV. The current traces in the absence and presence of AG879 were superimposed and the dashed line represents the current trace obtained by adjusting their peak amplitudes. (B) and (C) The effect of AG879 on the fast and slow inactivation time course. The inactivation time course of $K_v4.2$ currents were well fitted with a double-exponential function (n = 5). (D) Rate of open-channel block ($1/\tau_{block}$) as a function of the drug concentration.

larized to +40 mV once every 5 s from a holding potential –80 mV, AG879 not only caused a reduction in the peak current of $K_v4.2$/KChIP2 (Figure 1D) but also preferentially accelerated the inactivation rate. As a measurement of the peak current underestimates the steady-state compound effect on the $K_v4.2$ channels, we measured the integrated area of Kv4.2 current during the entire time of depolarization. IC_{50} values for AG879 to block the peak and the integrated $K_v4.2$/KChIP2 currents were 17.87 ± 1.75 μM, with Hill coefficient 0.72 ± 0.06, and 4.68 ± 0.61 μM, with Hill coefficient 0.86 ± 0.10, respectively. The inhibitory effect of AG879 on the $K_v4.2$/KChIP2 current was reversible (Figure 1E). AG879 also induced a similar level of inhibition on $K_v4.3$channels, a close family member of the $K_v4.2$ potassium channel, with IC_{50} value 14.94 ± 1.69 μM for peak current and 4.14 ± 0.16 μM for integrated current respectively (Figure 1F). However, AG879 10 μM did not have a significant effect on the other voltage-gated potassium channels $K_v1.1$, $K_v1.3$, $K_v1.4$, $K_v1.5$ and $K_v2.1$ (Supporting Information Figure S3). In addition, we investigated the mechanism of action of tyrphostin AG879 on $K_v4.2$/KChIP2 channels.

AG879 facilitated the inactivation of $K_v4.2$ channels

As shown in Figure 2A, the peak values of the control and AG879-blocked currents were set equal to 1; a very pronounced feature induced by AG879 was the increase in the inactivation rate of $K_v4.2$/KChIP2 channels during depolarization, which suggests an open-channel block mechanism (Hatano *et al.*, 2003). As described previously (Caballero *et al.*, 2003; Hatano *et al.*, 2003), the inactivation time course was fitted to a double exponential equation:

$$I(t) = A_{fast}\exp(-t/\tau_{fast}) + A_{slow}\exp(-t/\tau_{slow}) + A_0$$

where A_{fast} and τ_{fast} and A_{slow} and τ_{slow} are the initial amplitudes and time constants of the fast and slow components of inactivation, respectively; and A_0 is a time-independent component. The fast component of the inactivation current was predominant at +40 mV in control cells, with a relative contribution of 87% (determined as $A_{fast}/(A_{fast} + A_{slow})$). Therefore, the inactivation rate of $K_v4.2$-mediated currents was mainly determined by τ_{fast} under control conditions. The fast inactivation time constant at +40 mV was significantly decreased from a control value of 45.8 ± 2.70 ms (n = 10) to 13.57 ± 1.07 ms after AG879 20 μM treatment (*P << 0.01) (Figure 2B). The contribution of the fast component was significantly increased by AG879 to 99%. However, the slow inactivation time constant was not altered significantly (Figure 2C). Further experiments demonstrated that AG879 also accelerated the inactivation rate of $K_v4.2$ channels in the absence of KChIP2. Therefore, the increased inactivation rate of $K_v4.2$ channels by AG879 was

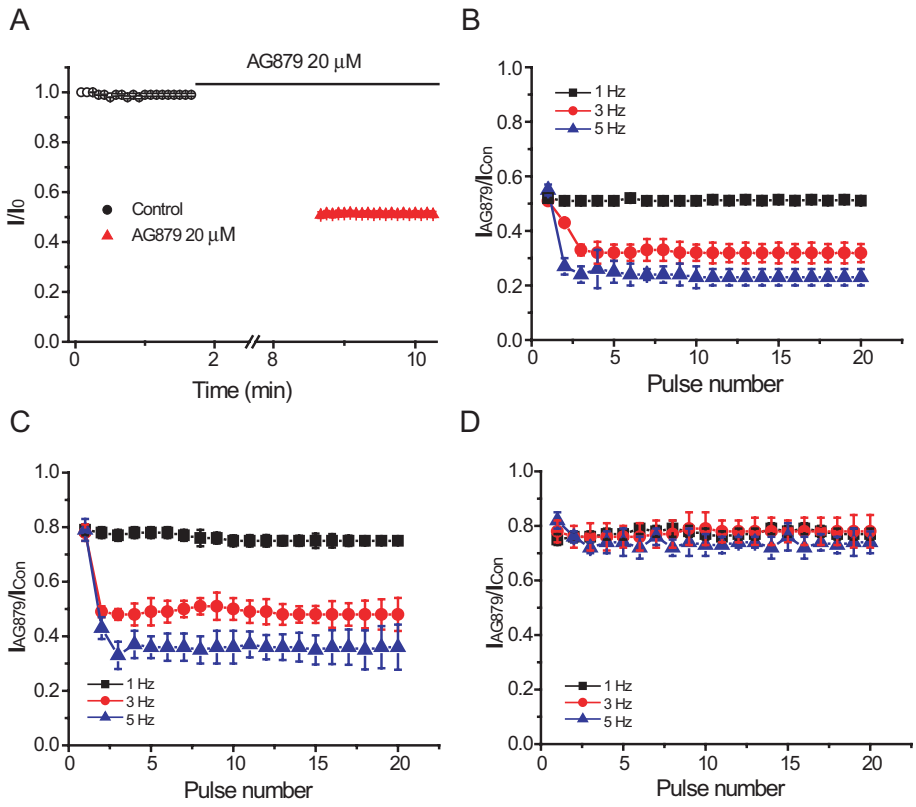

Figure 3

Use-dependent block by AG879 of $K_v4.2$ currents. (A) $K_v4.2$ currents were recorded with 0.2 Hz of 20 depolarization pulses from –80 to +40 mV and peak current change is shown in (A) before and after 7 min of incubation with AG879 20 μM, membrane potential held at –80 mV. (B) The peak amplitude of $K_v4.2$ at each pulse in the presence of AG879 was normalized to the corresponding one in the absence for 1, 3 and 5 Hz with holding potential at –80 mV. And then the ratios were plotted against the pulse number (n = 4–7). (C) Peak current changes for the different frequencies, 1, 3 and 5 Hz, after cells were loaded with AG879 for 7 min and then washed out, with membrane potential held at –80 mV. (D) Peak current changes for the different frequencies, 1, 3 and 5 Hz, after cells were loaded with AG879 for 7 min and then washed out, with membrane potential held at –100 mV.

independent of the KChIP2 subunit (Supporting Information Figure S4).

Based on the rate of inactivation, we further calculated the rate of open-channel block. As reported in the methods (Slawsky and Castle, 1994; Hatano *et al.*, 2003), the time constant for decay of $K_v4.2$ ($1/\tau_{decay}$) in the presence of a drug should reflect the sum of the time constants of channel inactivation ($1/\tau_{inactivation}$) and of open-channel block($1/\tau_{block}$) as follows: $1/\tau_{decay} = 1/\tau_{block} + 1/\tau_{inactivation}$. The time constant of fast inactivation was used to represent the $\tau_{inactivation}$ considering its predominant role in the inactivation of the $K_v4.2$ channel. The rate of open-channel block ($1/\tau_{block}$) was plotted against AG879 concentration (Figure 2D), and the data were well fitted by a line with the least squares linear fit: $1/\tau_{block} = \kappa_{+1}[D] + \kappa_{-1}$, where the association rate constant (κ_{+1}) is 2.43 ± 1.17 $\mu M^{-1}\cdot s^{-1}$, and the dissociation rate constant κ_{-1} = 2.24 ± 0.19 s^{-1}. The K_d (κ_{-1}/κ_{+1}) was estimated to be 0.92 μM, which was in reasonable agreement with the IC_{50} value of 4.68 μM derived from the concentration–response curve shown in Figure 1. These results also imply that AG879 inhibited the $K_v4.2$/KChIP2 channels through an open-channel block mechanism.

Use and frequency-dependent block of $K_v4.2$ channels

When the cells were exposed to AG879 20 μM for 5~7 min, the inhibition of peak current amplitude reached a plateau with the depolarization at 0.2 Hz (Figure 3A). The inhibition for the first pulse was identical to that of 20th pulse (0.50 ± 0.01 and 0.51 ± 0.01, $P > 0.05$), and no use-dependence was observed. The frequency-dependence of the AG879 block was further examined at 1, 3 and 5 Hz respectively. In the absence of AG879, 20 depolarizing pulses for 200 ms in duration from –80 to +40 mV were applied at 1, 3 and 5 Hz; the peak amplitude from the first to the 20th pulse was not changed significantly at 1 Hz. However, it was significantly decreased at 3 and 5 Hz, suggesting a frequency-dependent increase in inactivation. The relative amplitude ratios for the inhibition caused by AG879 20 μM at the first pulse were apparent with 0.51 ± 0.01, 0.51 ± 0.01 and 0.55 ± 0.02 for 1, 3 and 5 Hz respectively. The inhibitory effect showed no progressive change at 1 Hz, tended to increase at 3 Hz ($P < 0.05$, blocking effect between first and 20th pulses), and significantly increased at 5 Hz ($P < 0.01$). The relative amplitudes of the

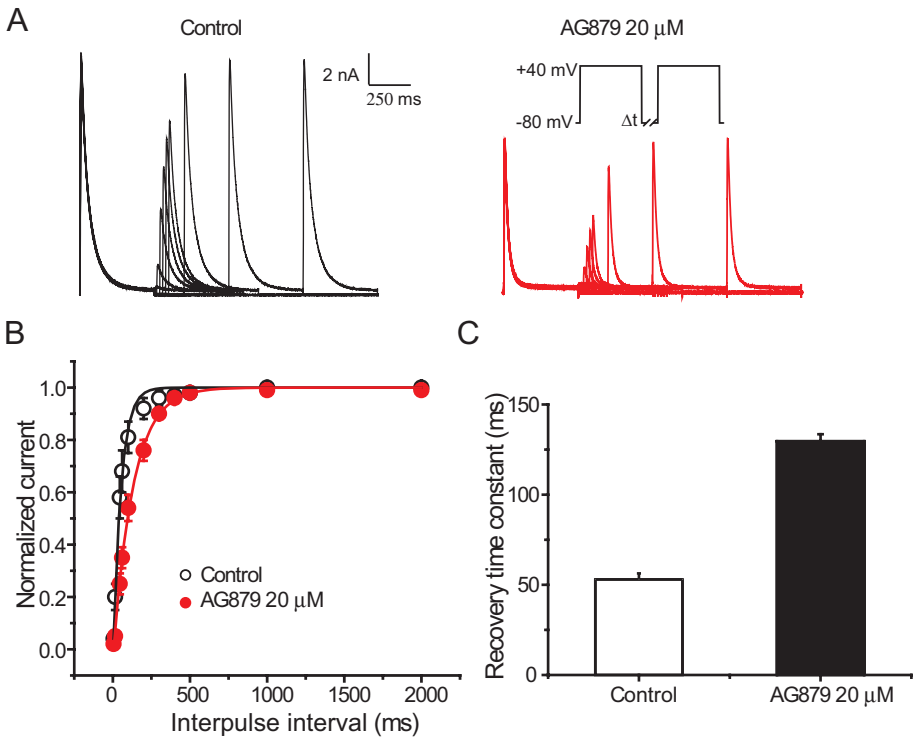

Figure 4

Effect of AG879 on the recovery from inactivation of $K_v4.2$ channels. (A) A double-pulse protocol was used to characterize the recovery of $K_v4.2$ channels from inactivation in the absence and presence of AG879. A pre-pulse of 500 ms depolarization to +40 mV from holding potential –80 mV was followed by a test pulse with 500 ms depolarization to +40 mV by increasing the inter-pulse duration from 10 to 2000 ms at –80 mV. The protocol is shown in the insert. (B) Peak current amplitude at the test pulse was normalized to that recorded from the conditioning pulses in the same cells. (C) Normalized data were plotted against the inter-pulse duration and fitted by a single exponential function. Data are expressed as mean ± SEM (n = 6).

inhibition at the 20th pulse were 0.51 ± 0.02, 0.32 ± 0.03 and 0.23 ± 0.03, indicating a strong use-dependent inhibition of $K_v4.2$ by AG879 (Figure 3B).

After the cell was exposed to AG879 20 μM for 7 min with the holding potential at –80 mV, the compound was washed out before the channel was activated (1, 3 and 5 Hz). Under these conditions, the use-dependent block could still be observed for 3 and 5 Hz, but not 1 Hz (Figure 3C). Theoretically, no use-dependent block should be observed in the no-channel-opened state. One interpretation is that there were a certain amount of $K_v4.2$ channels inactivated at the holding potential –80 mV, thus AG879 could access the inactivated channels to block the channel activity. Therefore, the holding potential was set to a more hyperpolarized voltage, –100 mV, to drive all the channels to a closed state. Under these conditions, no use- dependent block was observed for the different frequencies of depolarization (1, 3 and 5 Hz) after treatment with AG879 for 7 min and then washed out (Figure 3D). In contrast, when the cells were incubated with AG879 for a longer duration and then activated, the use-dependent inhibitory effect was restored. These experiments indicate that the inhibitory effect of AG879 on $K_v4.2$ channels was state-dependent.

Slowed recovery from inactivation of $K_v4.2$ channels by AG879

A double-pulse protocol was used to characterize the recovery of $K_v4.2$ channels from inactivation in the absence and presence of AG879 20 μM (as shown in Figure 4A). Peak current amplitude at the test pulse was normalized to that elicited by the conditioning pulses in the same cells. The normalized current amplitude was plotted against the inter-pulse durations. The time course for recovery from inactivation was well fitted by a single exponential function with a time constant of 53.0 ± 3.4 ms under control conditions and 129.6 ± 3.35 ms (n = 5, P < 0.01) in the presence of AG879 (Figure 4B and 4C). AG879 significantly slowed the recovery from inactivation of the $K_v4.2$ channel.

Voltage-dependent block of $K_v4.2$ channels by AG879

Current–voltage relationships were examined in the CHO-K1 cells expressing $K_v4.2$/KChIP2 in the absence or presence of AG879. $K_v4.2$-mediated currents were generated by depolarizing the cells from holding potential –80 mV to a series of voltage steps ranging from –70 to +70 mV for 300 ms in 10 mV increments and activated at voltage potentials more

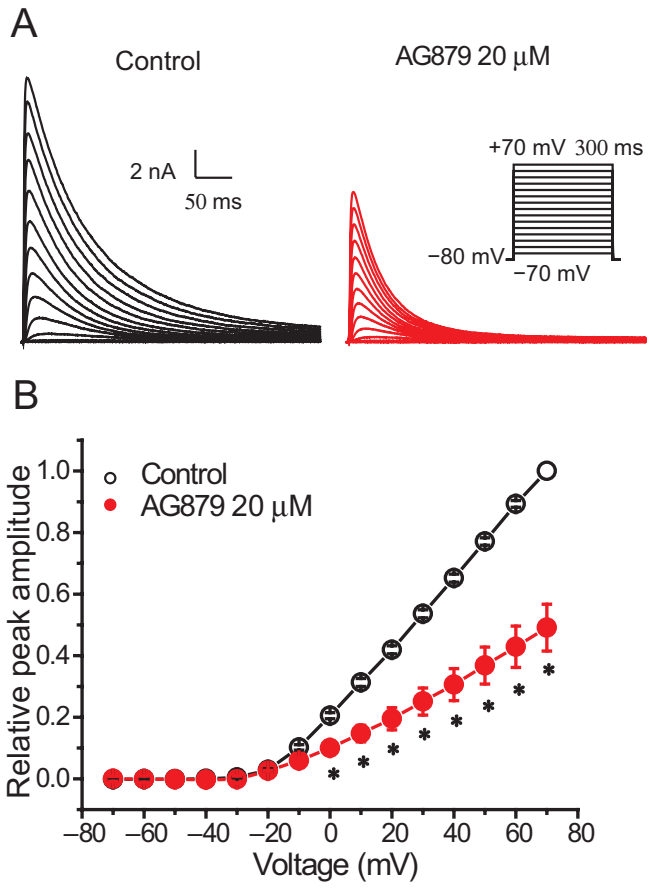

Figure 5

Effect of AG879 on current–voltage relationships of $K_v4.2$ channels in CHO-K1 cells. (A) Representative $K_v4.2$ channel current traces in the absence and presence of AG879 20 μM. Each CHO-K1 cell expressing $K_v4.2$ channels was depolarized for 300 ms from a holding potential of −80 mV in 10 mV increments, at 5 s intervals. (B) Current–voltage curves for peak current amplitude in the absence and presence of AG879 20 μM (n = 5). In each cell, the current amplitude measured at the peak current was normalized to that at +70 mV in the absence of AG879. Data are expressed as mean ± SEM (*P << 0.01).

than −30 mV (Figure 5A).The current–voltage relationships for peak currents are shown in Figure 5B. AG879 significantly reduced the amplitude of the $K_v4.2$-mediated peak current in the voltage range from 0 to +70 mV (*, P << 0.01).

To determine the voltage-dependent activation of $K_v4.2$ channels, the normalized tail currents were fitted to a Boltzmann function. AG879 induced a slight hyperpolarizing shift of the voltage-dependence, in which the half maximal activation voltage ($V_{1/2}$) was leftward shifted for 3.5 mV from control –0.40 ± 1.21 mV (mean ± SEM) to –3.92 ± 1.24 mV (Figure 6A and B). These results indicate that AG879 does not markedly change the voltage-dependence of the steady-state activation of $K_v4.2$ channels. To quantify the inhibitory effect of AG879, the relative current amplitudes for peak currents were plotted against test potentials. As shown in Figure 6C, the inhibitory effect induced by AG879 was increased steeply in the voltage range from –30 to +0 mV, when the $K_v4.2$ channels were in the unsaturated open status according to the activation curve (as shown in the dashed line in Figure 6C).The voltage-dependence of the block was determined at the potentials in the range of full channel opening (between +10 and +70 mV). The Woodhull model was used to generate fractional electrical distance δ = 0.10 ± 0.01 (Woodhull, 1973), suggesting a mild voltage-dependent inhibition.

Steady-state inactivation was examined using a double-pulse protocol as shown in the inset of Figure 6D. The half inactivation voltage was –45.68 ± 0.29 mV under control conditions with a slope of 5.09 ± 0.32. In the presence of AG879, the $V_{1/2}$ was shifted in a hyperpolarizing direction of ~6 mV ($V_{1/2}$ = –51.56 ± 0.80 mV and slope 5.30 ± 0.36). The blocking effect was plotted against the pre-pulse potentials as shown in Figure 6E; it remained at a relative stable level at potentials between –110 mV (23.30 ± 11.96%) and –60 mV (32.13 ± 10.47%, n = 5, P > 0.05). At more positive voltages, the blocking effect was enhanced as the number of inactivated channels increased, reaching a maximum at the pre-pulse voltage –40 mV (62.57 ± 8.7%, P < 0.01 vs. blocking effect at –110 mV).

Inhibition of A-type potassium currents by AG879 in hippocampus neurons

In the cultured hippocampal neurons the transient A-type current component (I_A) was separated from the total outward currents by a pre-pulse inactivation and subtraction protocol. Briefly, starting from a holding voltage of –80 mV, currents were activated at +40 mV, either following a 500 ms pre-pulse to –110 mV to obtain the total neuronal outward K current, or following a 500 ms pre-pulse to –30 mV to obtain the non- or slowly-inactivating delayed rectifier current I_D. The I_D component was then subtracted offline from the total neuronal outward K current in a point-by-point fashion to obtain I_A (Figure 7A). As shown in Figure 7A and 7B, AG879 20 μM significantly inhibited A-type potassium currents by around 55% in the cultured hippocampus neurons, comparable with the inhibition by AG879 of the current mediated by recombinant $K_v4.2$/KChIP2 channels.

Discussion and conclusions

In the present study, we identified tyrphostin AG879, a tyrosine kinase inhibitor, as a selective inhibitor of K_v4 channels. The main findings of the present study can be summarized as follows. AG879 selectively inhibited both $K_v4.2$/KChIP2 and $K_v4.3$ channels dose-dependently without a significant effect on the other voltage-gated potassium channels. The fast inactivation of $K_v4.2$ channels was significantly accelerated by AG879 in a KChIP2-independent manner. AG879 inhibited $K_v4.2$ currents in a use-dependent manner and also slowed their recovery from inactivation. Furthermore, AG879 induced a hyperpolarizing shift in the voltage-dependence of the steady-state inactivation of $K_v4.2$ channels. AG879 also exhibited apparent inhibition of the A-type potassium currents in cultured hippocampus neurons.

KChIPs co-localize with brain K_v4 α-subunits and are integral components of the native K_v4 channel complex (An

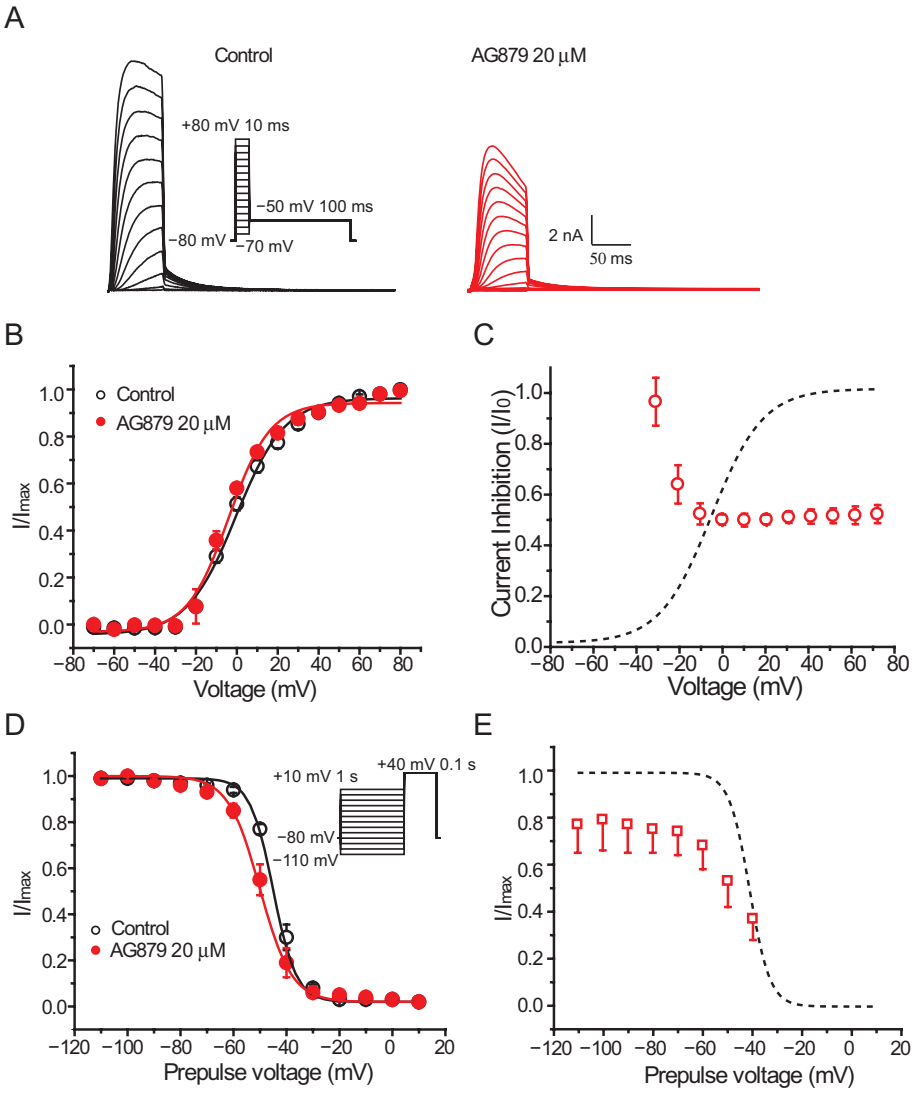

Figure 6

Effect of AG879 on the steady-state activation and inactivation of $K_v4.2$ channels. (A)The representative tail current traces of $K_v4.2$ channels in the absence and presence of AG879. Depolarized voltage steps from −70 to +80 mV were applied from a holding potential of −80 mV for 10 ms in 10 mV increments, followed by a hyperpolarizing step to −50 mV for 500 ms to record tail currents. (B) The activation curves in the absence and presence of AG879. The curves were well fitted to the Boltzmann equation. Data are expressed as mean ± SEM (n = 8). (C) Fraction block by 20 μM AG879 of the peak currents was plotted against the membrane potentials. The current amplitude in the presence of AG879 20 μM was normalized to that at each voltage in the absence of AG879 (control cells n = 5). (D) Inactivation curves in the absence and presence of AG879. The steady-state curves were generated with a two-pulse protocol, in which 1 s conditioning pulses from a holding potential of −80 mV to voltages between −110 and +10 mV in 10 mV increments were followed by a test pulse to +40 mV for 500 ms. (E) Fraction block was plotted as a function of the voltage from the preceding pulse.

et al., 2000). To mimic the native channel complex, we co-transfected the cDNAs of $K_v4.2$ and KChIP2 channels to study the effect of AG879. For the activation kinetics of the $K_v4.2$ channel, the peak current reflects the open state of the channel and the rest of the current reflects the steady state of equilibrium between open and inactivated states. As a measurement of the peak current would underestimate steady-state compound effect on the $K_v4.2$ channels, we also measured the integrated area of $K_v4.2$ currents for the entire time of depolarization. AG879 blocked $K_v4.2$/KChIP2-mediated currents in a dose-dependent manner. The IC_{50} values were 17.87 and 4.68 μM for the reduction of the peak current and integrated current respectively. In addition, AG879 also displayed a similar affinity for blockade of $K_v4.3$ channels. It is not too surprising that AG879 blocked both $K_v4.2$ and $K_v4.3$ channels because there is a high percentage of sequence identity between $K_v4.2$ and $K_v4.3$ channels (99% in pore region and 92% in voltage-sensor domain S1–S4). However, AG879 did not inhibit the other K_v channels tested ($K_v1.1$, $K_v1.3$, $K_v1.4$, $K_v1.5$ and $K_v2.1$). In addition, KChIP2 not only increased the current density, but also slowed the inactivation rate when co-expressed with the $K_v4.2$ channels;

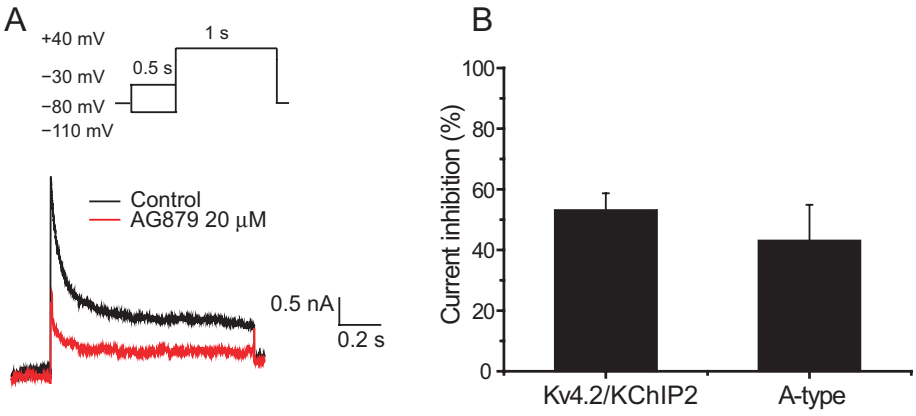

Figure 7

Effect of AG879 on A-type potassium currents in cultured hippocampus neurons. (A) Isolated A-type current from a cultured hippocampal neuron in the absence (upper trace) and presence of 20 μM AG879 (lower trace).(B) Bar chart plot for the inhibition of the peak current amplitude of K_v4.2/KChIP2 and A-type currents in the presence of AG879 (n = 5).

AG879 accelerated the inactivation rate of K_v4.2/KChIP2 channels. To determine whether AG879 attenuates the KChIP2-mediated slowing of inactivation of the K_v4.2 channels, we tested the effect of AG879 on the K_v4.2 inactivation rate in the absence of KChIP2 expression. The results demonstrated that the AG879-induced effects are independent of the KChIP2 subunit.

AG879 induced about a 20% block of the current in the resting state of K_v4.2 channels. However, its inhibitory effect was greatly enhanced when the channels were stimulated/activated, so that it accelerated inactivation or current reduction, which indicates that AG879 might interact with either the open state or the inactivated state. The characteristics of the AG879-induced blockade of K_v4.2 channels were also compared with those of other drugs that have been shown to affect either K_v4 channels or I_{to} channels in heart tissue (Slawsky and Castle, 1994; Wang *et al.*, 1995; Caballero *et al.*, 2003; Hatano *et al.*, 2003). Results with drugs such as flecanide, quinidine, nicardipine and propafenone that inhibit either cardiac I_{to} or K_v4 channels have been interpreted as indicative of them acting by an open-channel block mechanism. An important common characteristic of these agents and AG879 is the prominent acceleration of the inactivation rate. However, there are also differences in some aspects by which these drugs affect the channels. For example, the inhibition produced by quinidine on K_v4.2 and I_{to} channels is dependent on the test potential; however, the inhibition by AG879, as well as that induced by nicardipine and flecainide, was only slightly dependent on the test potential. In addition, unlike propafenone, AG879, flecainide, quinidine and nicardipine all generated use-dependent block at higher frequencies of stimulation. These were also associated with a slower recovery from inactivation for the time course of K_v4.2 and I_{to} channels.

K_v4.2 channels can be inactivated from the open state at strongly depolarized voltages or directly from closed states at more negative potentials (Bahring *et al.*, 2001). The peak current amplitude was significantly decreased from the first pulse to the 20th pulse while the stimulation frequencies were increased from 1 to 3 and 5 Hz, suggesting that the fraction of inactivated channels was increased. AG879-induced inhibition was also increased at higher frequencies of stimulation. In addition, we also observed that AG879 reduced the K_v4.2-mediated current use-dependently even though the channel was in a closed/inactivated state (membrane potential −80 mV). In addition, AG879 caused a hyperpolarizing-shift of the inactivation curve and its inhibitory effect became more pronounced as the fraction of inactivated channels increased. These results suggest it interacts with an inactivated-state or it accelerates the inactivation. More direct experiments, such as excised patch recordings and site-directed mutagenesis to knock-down or cancel the inactivation property of the channel, are needed to unravel the precise mechanisms of the compound.

Tyrphostin AG879 has long been widely used as a protein tyrosine kinase inhibitor and is known to have beneficial anti-tumour properties, which include inhibition of NGF-induced PLC-γ 1 phosphorylation and PI3K activation (Ohmichi *et al.*, 1993; Rende *et al.*, 2000; 2006), inhibition of ErbB2 receptors and the VEGF receptor 2 (FLK-1) (He *et al.*, 2001; 2004; Zhou and Brattain, 2005; Lee *et al.*, 2008) and indirect inhibition of the MAPK cascade (Gil *et al.*, 2003; Larsson, 2004). Although AG879 potently inhibits, with an IC_{50} of 1 μM, the expression of human epidermal growth factor receptor 2/ErbB2 receptors, the compound starts to cause apoptosis or reduce the proliferation of cells at concentrations more than 5–20 μM in TrkA-highly expressed tumour cell lines (Rende *et al.*, 2006). In our study, tyrphostin AG879 was identified as a selective inhibitor of K_v4.2 channels with an IC_{50} value similar to that of the above-mentioned concentrations. It has been reported that ion channels can be modulated by tyrosine kinase inhibitors (Son *et al.*, 2013). To differentiate any tyrosine kinase-dependent actions of AG879 from those induced by direct inhibition of K_v4.2 channels, a structurally dissimilar broad-spectrum tyrosine kinase inhibitor, genistein 30 μM, was pre-applied before the addition of AG879. AG879 20 μM could still inhibit the peak current mediated by K_v4.2 channels by around 70% after the tyrosine kinase activity had been completely inhibited by genistein (Supporting Information Figure S5). If AG879 inhibited the

K_v4.2-mediated currents by decreasing tyrosine kinase activity, pre-application of a broad-spectrum tyrosine kinase inhibitor, such as genistein, would reduce or prevent the further inhibition of the current mediated by K_v4.2 channels induced by AG879. However, our results do not support this. Furthermore, if the AG879-induced inhibitory effect was dependent on tyrosine kinase, it would be weakened or cancelled when a protein phosphatase inhibitor was co-applied, as reported previously (Li *et al.*, 2006; Gierten *et al.*, 2008; Zhang *et al.*, 2012). However, an effective concentration of orthovanadate, an inhibitor of protein phosphates (Swarup *et al.*, 1982), did not reverse the inhibitory effect of AG879 (Supporting Information Figure S5). All these results indicate that the tyrosine-phosphorylation pathway is not involved in the process of AG879-induced channel inhibition and that AG879's inhibition of the K_v4.2 channel is unlikely to be mediated by an effect on tyrosine kinase. However, although our results revealed a PTK-independent modulation by AG879 of K_v4.2/KChIP2, we cannot completely rule out the possibility that this compound might inhibit the channel via a tyrosine-phosphorylation sensitive pathway, which is secondary to the direct interaction.

A-type currents play an important role in the shaping of an action potential and regulate the firing frequency of neurons in the CNS (Rudy, 1988). K_v4.2 is the major contributing subunit for I_A in the CNS and plays an important role in modulating synaptic activity, influencing hippocampus-dependent tasks and neuronal excitability. AG879 caused significant inhibition of I_A currents in cultured hippocampus neurons. Inhibition of neuronal A-type currents would affect the refractory period and the action potential duration, and further alter the firing frequency of neurons. Furthermore, K_v4.2 inhibitors can restore the deficits in LTP induced in the FMR1 KO mice model (Lee *et al.*, 2011). Thus pharmacological inhibition of K_v4.2 currents by AG879 or similar compounds may have potential as a treatment for individuals with Fragile X syndrome.

In summary, the results of the present study suggest that AG879 selectively and directly inhibits K_v4.2/K_v4.3 channels by preferentially interacting with or stabilizing the open/inactivated states. Furthermore, this inhibitory effect of AG879 is not mediated through inhibition of PTK activity. It should be noted that K_v4.2 potassium channels are also expressed in heart tissue (Barry *et al.*, 1995) and the corresponding cardiac safety issues might be an issue if AG879 is used *in vivo*. Therefore, we recommend caution in the use of the drug in physiological experiments designed to determine the role of PKs in the modulation of ion channels. However, AG879 selectively inhibited K_v4.2 and K_v4.3 channels with no apparent effect on the other K_v channels tested. AG879 may have potential as a tool to study the role of neuronal A-type currents, especially K_v4.2 channels, in Fragile X syndrome in the CNS.

Acknowledgements

This work was supported by the start-up fund from the Institute of Materia Medica, Chinese Academy of Medical Sciences and Peking Union Medical College (to H. Y.) and by National Institutes of Health and Molecular Libraries Probe Production Centers Network (MLPCN) Grants U54MH084691 (to M. L.), and Johns Hopkins University is a member of the MLPCN and houses the Johns Hopkins Ion Channel Center.

Author contributions

H. Y. designed the experiments, analysed data and wrote the paper. B. Z. performed the experiments and analysed data. X. W. contributed new reagents/analytical tools. M. L. designed the experiments and revised the paper.

Conflict of interest

None.

References

Ahlemeyer B, Baumgart-Vogt E (2005). Optimized protocols for the simultaneous preparation of primary neuronal cultures of the neocortex, hippocampus and cerebellum from individual newborn (P0.5) C57Bl/6J mice. J Neurosci Methods 149: 110–120.

Alexander SPH, Benson HE, Faccenda E, Pawson AJ, Sharman JL, Spedding M *et al.* (2013a). The Concise Guide to PHARMACOLOGY 2013/14: ion channels. Br J Pharmacol 170: 1607–1651.

Alexander SPH, Benson HE, Faccenda E, Pawson AJ, Sharman JL, Spedding M *et al.* (2013b). The Concise Guide to PHARMACOLOGY 2013/14: catalytic receptors. Br J Pharmacol 170: 1676–1705.

An WF, Bowlby MR, Betty M, Cao J, Ling HP, Mendoza G *et al.* (2000). Modulation of A-type potassium channels by a family of calcium sensors. Nature 403: 553–556.

Bahring R, Boland LM, Varghese A, Gebauer M, Pongs O (2001). Kinetic analysis of open- and closed-state inactivation transitions in human Kv4.2 A-type potassium channels. J Physiol 535 (Pt 1): 65–81.

Barry DM, Trimmer JS, Merlie JP, Nerbonne JM (1995). Differential expression of voltage-gated K+ channel subunits in adult rat heart. Relation to functional K+ channels? Circ Res 77: 361–369.

Birnbaum SG, Varga AW, Yuan LL, Anderson AE, Sweatt JD, Schrader LA (2004). Structure and function of Kv4-family transient potassium channels. Physiol Rev 84: 803–833.

Caballero R, Pourrier M, Schram G, Delpon E, Tamargo J, Nattel S (2003). Effects of flecainide and quinidine on Kv4.2 currents: voltage dependence and role of S6 valines. Br J Pharmacol 138: 1475–1484.

Chen X, Yuan LL, Zhao C, Birnbaum SG, Frick A, Jung WE *et al.* (2006). Deletion of Kv4.2 gene eliminates dendritic A-type K+ current and enhances induction of long-term potentiation in hippocampal CA1 pyramidal neurons. J Neurosci 26: 12143–12151.

Diochot S, Drici MD, Moinier D, Fink M, Lazdunski M (1999). Effects of phrixotoxins on the Kv4 family of potassium channels and implications for the role of Ito1 in cardiac electrogenesis. Br J Pharmacol 126: 251–263.

Ebbinghaus J, Legros C, Nolting A, Guette C, Celerier ML, Pongs O *et al.* (2004). Modulation of Kv4.2 channels by a peptide isolated from the venom of the giant bird-eating tarantula *Theraphosa leblondi*. Toxicon 43: 923–932.

Gierten J, Ficker E, Bloehs R, Schlomer K, Kathofer S, Scholz E *et al.* (2008). Regulation of two-pore-domain (K2P) potassium leak channels by the tyrosine kinase inhibitor genistein. Br J Pharmacol 154: 1680–1690.

Gil C, Chaib-Oukadour I, Aguilera J (2003). C-terminal fragment of tetanus toxin heavy chain activates Akt and MEK/ERK signalling pathways in a Trk receptor-dependent manner in cultured cortical neurons. Biochem J 373 (Pt 2): 613–620.

Hatano N, Ohya S, Muraki K, Giles W, Imaizumi Y (2003). Dihydropyridine Ca2+ channel antagonists and agonists block Kv4.2, Kv4.3 and Kv1.4 K+ channels expressed in HEK293 cells. Br J Pharmacol 139: 533–544.

He H, Hirokawa Y, Manser E, Lim L, Levitzki A, Maruta H (2001). Signal therapy for RAS-induced cancers in combination of AG 879 and PP1, specific inhibitors for ErbB2 and Src family kinases, that block PAK activation. Cancer J 7: 191–202.

He H, Hirokawa Y, Gazit A, Yamashita Y, Mano H, Kawakami Y *et al.* (2004). The Tyr-kinase inhibitor AG879, that blocks the ETK-PAK1 interaction, suppresses the RAS-induced PAK1 activation and malignant transformation. Cancer Biol Ther 3: 96–101.

Hoffman DA, Magee JC, Colbert CM, Johnston D (1997). K+ channel regulation of signal propagation in dendrites of hippocampal pyramidal neurons. Nature 387: 869–875.

Hu HJ, Carrasquillo Y, Karim F, Jung WE, Nerbonne JM, Schwarz TL *et al.* (2006). The kv4.2 potassium channel subunit is required for pain plasticity. Neuron 50: 89–100.

Kilkenny C, Browne W, Cuthill IC, Emerson M, Altman DG (2010). Animal research: reporting *in vivo* experiments: the ARRIVE guidelines. Br J Pharmacol 160: 1577–1579.

Kim J, Wei DS, Hoffman DA (2005). Kv4 potassium channel subunits control action potential repolarization and frequency-dependent broadening in rat hippocampal CA1 pyramidal neurones. J Physiol 569 (Pt 1): 41–57.

Larsson LI (2004). Novel actions of tyrphostin AG 879: inhibition of RAF-1 and HER-2 expression combined with strong antitumoral effects on breast cancer cells. Cell Mol Life Sci 61: 2624–2631.

Lee HK, Seo IA, Lee SH, Seo SY, Kim KS, Park HT (2008). Tyrphostin ErbB2 inhibitors AG825 and AG879 have non-specific suppressive effects on gp130/ STAT3 signaling. Korean J Physiol Pharmacol 12: 281–286.

Lee HY, Ge WP, Huang W, He Y, Wang GX, Rowson-Baldwin A *et al.* (2011). Bidirectional regulation of dendritic voltage-gated potassium channels by the fragile X mental retardation protein. Neuron 72: 630–642.

Li SY, Huang BB, Ouyang S (2006). Effect of genistein on voltage-gated potassium channels in guinea pig proximal colon smooth muscle cells. World J Gastroenterol 12: 420–425.

Lugo JN, Brewster AL, Spencer CM, Anderson AE (2012). Kv4.2 knockout mice have hippocampal-dependent learning and memory deficits. Learn Mem 19: 182–189.

McGrath JC, Drummond GB, McLachlan EM, Kilkenny C, Wainwright CL (2010). Guidelines for reporting experiments involving animals: the ARRIVE guidelines. Br J Pharmacol 160: 1573–1576.

Norris AJ, Nerbonne JM (2010). Molecular dissection of I(A) in cortical pyramidal neurons reveals three distinct components encoded by Kv4.2, Kv4.3, and Kv1.4 alpha-subunits. J Neurosci 30: 5092–5101.

Ohmichi M, Pang L, Ribon V, Gazit A, Levitzki A, Saltiel AR (1993). The tyrosine kinase inhibitor tyrphostin blocks the cellular actions of nerve growth factor. Biochemistry 32: 4650–4658.

Pawson AJ, Sharman JL, Benson HE, Faccenda E, Alexander SP, Buneman OP *et al.*; NC-IUPHAR (2014). The IUPHAR/BPS Guide to PHARMACOLOGY: an expert-driven knowledgebase of drug targets and their ligands. Nucl Acids Res 42 (Database Issue): D1098–D1106.

Rende M, Brizi E, Conner J, Treves S, Censier K, Provenzano C *et al.* (2000). Nerve growth factor (NGF) influences differentiation and proliferation of myogenic cells *in vitro* via TrKA. Int J Dev Neurosci 18: 869–885.

Rende M, Pistilli A, Stabile AM, Terenzi A, Cattaneo A, Ugolini G *et al.* (2006). Role of nerve growth factor and its receptors in non-nervous cancer growth: efficacy of a tyrosine kinase inhibitor (AG879) and neutralizing antibodies antityrosine kinase receptor A and antinerve growth factor: an *in-vitro* and *in-vivo* study. Anticancer Drugs 17: 929–941.

Rudy B (1988). Diversity and ubiquity of K channels. Neuroscience 25: 729–749.

Sanguinetti MC, Johnson JH, Hammerland LG, Kelbaugh PR, Volkmann RA, Saccomano NA *et al.* (1997). Heteropodatoxins: peptides isolated from spider venom that block Kv4.2 potassium channels. Mol Pharmacol 51: 491–498.

Slawsky MT, Castle NA (1994). K+ channel blocking actions of flecainide compared with those of propafenone and quinidine in adult rat ventricular myocytes. J Pharmacol Exp Ther 269: 66–74.

Snyders J, Knoth KM, Roberds SL, Tamkun MM (1992). Time-, voltage-, and state-dependent block by quinidine of a cloned human cardiac potassium channel. Mol Pharmacol 41: 322–330.

Son YK, Park H, Firth AL, Park WS (2013). Side-effects of protein kinase inhibitors on ion channels. J Biosci 38: 937–949.

Swarup G, Cohen S, Garbers DL (1982). Inhibition of membrane phosphotyrosyl-protein phosphatase activity by vanadate. Biochem Biophys Res Commun 107: 1104–1109.

Truchet B, Manrique C, Sreng L, Chaillan FA, Roman FS, Mourre C (2012). Kv4 potassium channels modulate hippocampal EPSP-spike potentiation and spatial memory in rats. Learn Mem 19: 282–293.

Tseng GN, Jiang M, Yao JA (1996). Reverse use dependence of Kv4.2 blockade by 4-aminopyridine. J Pharmacol Exp Ther 279: 865–876.

Wang Z, Fermini B, Nattel S (1995). Effects of flecainide, quinidine, and 4-aminopyridine on transient outward and ultrarapid delayed rectifier currents in human atrial myocytes. J Pharmacol Exp Ther 272: 184–196.

Woodhull AM (1973). Ionic blockage of sodium channels in nerve. J Gen Physiol 61: 687–708.

Yuan W, Burkhalter A, Nerbonne JM (2005). Functional role of the fast transient outward K+ current IA in pyramidal neurons in (rat) primary visual cortex. J Neurosci 25: 9185–9194.

Zhang YH, Wu W, Sun HY, Deng XL, Cheng LC, Li X *et al.* (2012). Modulation of human cardiac transient outward potassium current by EGFR tyrosine kinase and Src-family kinases. Cardiovasc Res 93: 424–433.

Zhou Y, Brattain MG (2005). Synergy of epidermal growth factor receptor kinase inhibitor AG1478 and ErbB2 kinase inhibitor AG879 in human colon carcinoma cells is associated with induction of apoptosis. Cancer Res 65: 5848–5856.

Supporting information

Additional Supporting Information may be found in the online version of this article at the publisher's web-site:

http://dx.doi.org/10.1111/bph.13127

Figure S1 A pilot screening for $K_v4.2$ channel modulators in the LOPAC library using a thallium-influx assay.
Figure S2 Improved $K_v4.2$ potassium channel expression by accessory subunit KChIP2.
Figure S3 Effect of AG879 on K_v channels.
Figure S4 Effect of AG879 on the inactivation time course of $K_v4.2$ channels.
Figure S5 AG879 inhibited $K_v4.2$/KChIP2 channels in a TK insensitive manner.